RM L50L07

NACA

RESEARCH MEMORANDUM

AN EXPERIMENTAL STUDY AT MODERATE AND HIGH SUBSONIC SPEEDS OF THE FLOW OVER AN UNSWEPT WING IN CONJUNCTION WITH A FUSELAGE

By Richard T. Whitcomb

Langley Aeronautical Laboratory
Langley Field, Va.

NATIONAL ADVISORY COMMITTEE
FOR AERONAUTICS

WASHINGTON

June 18, 1951

NATIONAL ADVISORY COMMITTEE FOR AERONAUTICS

RESEARCH MEMORANDUM

AN EXPERIMENTAL STUDY AT MODERATE AND HIGH SUBSONIC SPEEDS OF THE FLOW OVER AN UNSWEPT WING IN CONJUNCTION WITH A FUSELAGE

By Richard T. Whitcomb

SUMMARY

Pressure distributions, wake measurements, and tuft patterns have been obtained for an unswept wing, in conjunction with a fuselage, at Mach numbers to 0.925. The wing has an NACA 65-210 section, an aspect ratio of 9.0, and a taper ratio of 0.4. A study of the results of these measurements indicates that when the angle of attack is increased at a Mach number of 0.60, separation occurs initially at the wing-fuselage juncture. Separation associated with the onset of shock is less severe on the sections of the wing near the tip and wing-fuselage juncture than on the midsemispan sections.

INTRODUCTION

To provide a basis for a further understanding of the flow over unswept and swept wings at moderate and high subsonic speeds, pressure distributions, tuft patterns, and wake measurements have been obtained for high-aspect-ratio, tapered wings with no sweep and 30° and 45° of sweepback and sweepforward, in conjunction with a typical fuselage. These measurements were made in the Langley 8-foot high-speed tunnel at Mach numbers from 0.6 to 0.96. A study of the measurements made for the unswept wing is presented herein. This study provides an insight into the nature of the relieving effects of the tip and fuselage. Similar studies for the sweptback and sweptforward wings are presented in references 1 and 2.

SYMBOLS

b	span of model
s	distance measured along quarter-chord line of wing from plane of symmetry
c	section chord perpendicular to quarter-chord line
l	distance from leading edge of wing
α	geometric angle of attack
M	Mach number
q	dynamic pressure, pounds per square foot $\left(\frac{1}{2}\rho V^2\right)$
V	velocity in undisturbed stream, feet per second
ρ	mass density in undisturbed stream, slugs per cubic foot
p	local static pressure at a point on airfoil or fuselage, pounds per square foot
p_o	static pressure in undisturbed stream, pounds per square foot
P	pressure coefficient, $\left(\frac{p - p_o}{q}\right)$
ΔH	total-pressure loss, pounds per square foot
c_n	section normal-force coefficient (coefficients for fuselage based on chord of wing extended through fuselage (fig. 1)) $\left(\frac{1}{c}\int_0^c \left(P_L - P_U\right)dl\right)$
c_{d_o}	wing-section profile-drag coefficient from wake-survey measurements

Subscripts:

L	lower surface
U	upper surface
cr	critical

APPARATUS

Wing models.- The configuration investigated is shown in figure 1. The wing has an NACA 65-210 section, an aspect ratio of 9.0, and a taper ratio of 0.4; it has no sweep, twist, or dihedral. The ordinates of the tip and the NACA 65-210 section are presented in reference 3. Two wing models were used in the investigation. One model, used to obtain the static-pressure data, incorporated 20 static-pressure orifices at each of eight stations along the wing span in lines perpendicular to the quarter-chord line. The rows of orifices, shown in figure 1, were at 11, 20, 30, 43, 56, 64, 80, and 95 percent of the semispan from the plane of symmetry. On the actual wing, the four outboard stations were placed on the left half of the wing, while the four inboard stations were placed on the right half. A 20-percent-chord, straight-sided aileron that extends from the 60-percent-semispan station to the end of the straight part of the trailing edge of the unswept wing as shown in figure 1 was incorporated in this model. The angle of the aileron was 0° for the investigation reported herein. The second wing model, used for the wake and tuft measurements, incorporated no pressure orifices or aileron.

Support.- The models were supported in the tunnel by means of a vertical steel plate, which is completely described in reference 3. This plate had a negligible effect on the data obtained.

Fuselage.- The effect of the addition of a fuselage to a complete wing was simulated by the addition of half bodies of revolution to the test configuration on both sides of the support plate. The dimensions of the half bodies of revolution, the center lines of which coincided with the chord plane of the wing, are shown in figure 1. Twenty-eight pressure orifices were placed in one of the halves of the fuselage in two planes at 45° to the plane of symmetry through the center line as shown in figure 1.

Survey apparatus.- Total and static pressure measurements were made at various vertical stations behind the wing by means of the rake shown in figure 2 and described in reference 4. Tufts of fine linen thread were attached to the surface of the wing and fuselage with Scotch cellulose tape.

Reynolds numbers.- The variation of Reynolds number with Mach number is presented in figure 3. The Reynolds numbers are based on the mean chord of the wing outboard of the fuselage.

RESULTS

Pressure distributions.- The distributions of pressure on the wing for a number of test conditions are presented in figure 4. Other pressure data obtained during the investigation are presented in reference 4. The distributions are presented in the form of contours of equal pressure coefficient on plan forms of the wing. The positions of pressure peaks are indicated by lines of short dashes. The locations of the rows of pressure orifices and the tenths of chords of the various stations are indicated by light lines of long dashes.

To indicate more explicitly the changes in pressure on the wing near the wing-fuselage juncture, pressure distributions in the stream direction at a station 0.25 fuselage radius from the surface of the fuselage are presented in figure 5. Pressure distributions obtained at the two streamwise rows of orifices on the surface of the fuselage are also presented in figure 5.

Spanwise variations in section normal-force coefficient c_n are presented in figure 6.

Tuft patterns and wake measurements.- Selected tuft patterns obtained on the upper and lower surfaces of the configuration are presented in figure 7. Generally, the tuft patterns are presented for the same Mach number and angle-of-attack conditions for which pressure contours are presented.

Some of the distributions of total-pressure loss in planes normal to the wing plane at various spanwise locations behind the wing are presented in figure 8. The spanwise variations of wing-section profile-drag coefficient at several Mach numbers at various angles of attack are presented in figure 9. These coefficients were obtained from total-pressure measurements by use of the method described in reference 5. The measurements of the distributions of total-pressure loss were made at stations 12.7, 18.0, 25.0, 50.0, 75.0, and 95.0 percent semispans from the support plane and 8.4 inches downstream of the 25-percent-chord line of the wing.

Corrections.- No corrections for the effects of tunnel-wall interference have been applied to the data presented. Estimations of the order of magnitude of these effects indicate that the corrections to be applied to dynamic pressures and Mach numbers for all conditions are less, and in most cases much less, than 1 percent. Only data relatively free from choking effects have been used in this study. A discussion of the limitations imposed by blockage interference near choking during the investigation is presented in reference 3.

DISCUSSION

In the following study, the flow over the wing and fuselage is considered primarily at angles of attack of 2° and 7°, although data were obtained at other conditions. Generally, the flow over the wing at other angles of attack is indicated by the data obtained for these two conditions.

Angle of Attack of 2° at a Subcritical Mach Number of 0.6

Pressure distributions.- Near the tip of the wing, for an angle of attack of 2° at a Mach number of 0.60, the negative pressure coefficients and the corresponding induced velocities at various regions on the upper surface are considerably less than those at corresponding points farther inboard (fig. 4(a)). As previously pointed out in reference 1, these differences can be attributed primarily to the reduction in the circulation around the tip sections associated with the tip vortex. It is also caused in part by the three-dimensional relieving effect at the tip as described in references 6 and 7.

Near the wing-fuselage juncture, the pressure coefficients at various points, except those near the leading edge of the upper surface, are considerably less negative than those on the same region of the wing when no fuselage is present (fig. 5(a)). This reduction may be attributed to a relieving effect of the fuselage on the flow around these sections. Near the leading edge of the upper surface of sections in the vicinity of the juncture, the pressure coefficients are more negative than those present in the same region when no fuselage is present (fig. 5(a)). A comparison of the pressure distributions presented with those for an angle of attack of -2°, for which the lift is nearly zero (reference 4), indicates that this effect is associated with the lift. The effect is a result of the mutual interference of the wing and fuselage. Because of the relieving effect of the fuselage, the region of these higher induced velocities is limited in chordwise and vertical extent (fig. 5(a)).

Boundary-layer losses.- The spanwise variations of section profile-drag coefficients for angles of attack of 2° and 4° at a Mach number of 0.60 (figs. 9(b) and 9(c)) indicate peaks in the boundary-layer losses at the wing-fuselage juncture. These peaks are believed to be due to the adverse pressure gradients near the leading edge of the wing sections near the juncture (fig. 4(a)) and to the interference of fuselage boundary layer on the wing boundary layer.

Angle of Attack of 2° at Mach Numbers Greater Than the Drag-Divergence Value

Drag-divergence Mach number.- On the basis of the peak negative pressure coefficient measured on the upper surface of the unswept wing at an angle of attack of 2° for a Mach number of 0.60 (fig. 4(a)), it has been estimated that the critical Mach number for this angle of attack is approximately 0.71. The drag coefficient for the wing starts to rise at a Mach number of approximately 0.73 (fig. 11 of reference 8).

Pressure distributions.- When the Mach number is increased beyond the drag-divergence value to 0.80 and 0.89 for an angle of attack of 2°, the changes in the magnitudes of pressure coefficients at various chordwise stations near the wing-fuselage juncture and near the tip on both the upper and lower surfaces are generally less pronounced than those for the midsemispan region (fig. 4). These smaller changes are believed to be primarily a result of the reduced separation in these regions (fig. 7(e)). Because of these less pronounced variations, at a Mach number of 0.89 the pressure coefficients at the various points on the upper surface of the sections near the juncture and tip are generally of the same magnitude as those at corresponding points in the midsemispan region, although they were generally more positive at subcritical speeds. The peak coefficients on the lower surfaces of these sections at a Mach number of 0.89 are generally more positive than those over the major central region.

When the Mach number is increased above the drag-divergence value, the changes in normal-force coefficients for these inboard and outboard sections are considerably less pronounced than the changes in the coefficients for the sections in the midsemispan region (fig. 6). At a Mach number of 0.89, the normal-force coefficients for these sections are greater than those for the midsemispan region. The losses in normal-force coefficient for these inboard and outboard sections, however, are greater than those which might be expected, considering the relatively small amount of separation in these regions (fig. 7(e)). This phenomenon is associated with the induced effects; the severe losses in the normal-force coefficients for the midsemispan region induce reductions in the coefficients for the inboard and outboard sections.

Shocks.- The wake measurements (fig. 8(a)) indicate the presence of a significant shock on the midsemispan region (18- to 50-percent semispan) of the upper surface of the wing at a Mach number of 0.80 for an angle of attack of 2°. (The strength of the shock is indicated by the magnitude of the total-pressure losses in the region above the boundary-layer wake.) At this Mach number of 0.80, no shock losses are perceptible behind the outboard sections or the sections near the fuselage. The apparent elimination or great reduction in shock strength in these regions is believed to be due primarily to the reduction of the induced velocities ahead of the

shock (fig. 4(b)). At the 18.0-percent-semispan station the shock is stronger than it is above the midsemispan sections (fig. 8(a)), even though the maximum velocities ahead of the shock in this region are no higher than they are farther outboard (fig. 4(b)). When the Mach number is increased to 0.89, the strength of the shock on the upper surface of the sections at and near the juncture (fig. 8(b)) greatly exceeds that for the sections in the midsemispan region, although the velocities ahead of the shock in this region are approximately the same as those farther outboard (fig. 4(c)). The shock on the tip sections is relatively weak even though the velocities ahead of the shock in this region are greater than those farther inboard (fig. 4(c)).

Separation.- When the Mach number is increased beyond the drag-divergence value to 0.89, the drag coefficients for the midsemispan sections increase by relatively large amounts (fig. 9(b)). Only a slight amount of separation exists, however, on the upper surface of the sections near the tip at supercritical Mach numbers up to the highest test value of 0.89. This fact is indicated by the small boundary-layer losses measured behind the 95-percent-semispan station (fig. 8(b)), the tuft patterns for sections near the tip (fig. 7(e)), and the very severe adverse pressure gradient and favorable pressure recoveries on the upper surface of the 95-percent-semispan station (fig. 4(c)). The reduction of separation on the outboard region of the upper surface may be due in part to the weaker shock in this region (fig. 8(b)) and in part to a stabilization of the boundary layer associated with the spanwise gradients of pressure or energy loss in the tip region.

The wake measurements and tuft patterns indicate that near the wing-fuselage juncture the separation on the upper surface is generally less severe than it is on the sections farther outboard, although the shock near the surface in this region is generally stronger than on these outer sections (fig. 8). The localized increase in the boundary-layer losses measured behind the 12-percent-semispan station at a Mach number of 0.80 (fig. 8(a)) is believed to be associated with the effect of the fuselage boundary layer on the wing boundary layer, as is the similar increase at a Mach number of 0.60.

The wake surveys (fig. 8(b)) for a Mach number of 0.89 and the tuft patterns (fig. 7(h)) for a Mach number of 0.925 indicate that there is little separation associated with the strong shock on the midsemispan region of the lower surface at these highest test Mach numbers. The negative pressures near the trailing edge of the lower surface (fig. 4(e)), similar to those usually associated with separation, may be due to the induced effect of the highly negative pressures near the trailing edge of the upper surface (fig. 4(c)).

The tuft patterns obtained on the upper surface at a Mach number of 0.925 for this angle of attack of 2° (fig. 7(f)) indicate that the

extent of separation on all sections decreases when the Mach number is increased to this value. At higher Mach numbers this trend probably continues.

Angle of Attack of 7° at a Mach Number of 0.6

Separation.- The tuft patterns (fig. 7(i)) indicate that there is no perceptible separation associated with the high supersonic velocities and shock near the leading edge of the upper surface of the midsemispan and outboard sections (fig. 4(f)) for this angle of attack of 7° at a Mach number of 0.6.

The wake measurements (fig. 9(d)), tuft patterns, and pressure distributions for this condition indicate that the flow over the upper surface of the sections near the juncture separates perceptibly. The wake measurements indicate that the maximum amount of low-energy air due to this separation leaves the trailing edge somewhat outboard the juncture. This behavior would be expected since the severe spanwise pressure gradients near the juncture redirect this low-energy air outward as indicated by the tuft patterns. This separation is due to a pronounced increase in the pressure peak present near the juncture at an angle of attack of 2° (fig. 4(a)), when the angle is increased (reference 4). The pressure peak is greatly reduced when the angle is increased beyond that of initial separation.

Angle of Attack of 7° at a Mach Number of 0.8

Pressure distributions.- When the Mach number is increased from 0.6 to 0.8 for an angle of attack of 7°, the magnitude of the changes of the pressure distributions on the sections near the tip and fuselage are less severe than they are for the sections in the midsemispan region. Near the fuselage, the peak negative pressure coefficient is considerably greater than that on the sections farther outboard. This difference may be attributed to the mutual interference of wing and fuselage.

As at lower angles, there is a gradual deceleration of the highly supersonic flow ahead of the severe adverse pressure gradients associated with the shock on the upper surface of the wing. At the midsemispan and outboard sections, this deceleration may be attributed to the effect of positive pressure disturbances traveling forward in the region of separated flow (reference 9) and to the spanwise induced effects associated with such a flow. Near the wing-fuselage juncture the adverse pressure gradients ahead of the shock are considerably more severe than for sections farther outboard. The greater deceleration in this region cannot be attributed entirely to disturbances moving forward in the

low-speed separated boundary layer, since the separation in this region is less pronounced than it is farther outboard. It may be caused by the induced effects of the fuselage on the flow above the wing.

Shocks.- Except near the wing-fuselage juncture, the spanwise variation of the strength of the shock above the upper surface of the wing for an angle of attack of 7° at a Mach number of 0.80 (fig. 8(c)) is generally similar to that for an angle of attack of 2° at a Mach number of 0.89 (fig. 8(b)). On the outboard sections the shock is considerably weaker than it is in the midsemispan region, while somewhat outboard of the juncture, 18-percent-semispan station, the shock is stronger than in this midsemispan region. However, the shock at this angle of attack is considerably stronger at the various stations than is the shock at 2°. As at the lower angle of attack, the weaker shock near the tip cannot be attributed to the reduction of the maximum induced velocities in this region.

For the condition under consideration, the shock near the fuselage, 12.7-percent-semispan station, is weaker than it is slightly farther outboard, although at an angle of attack of 2° for a Mach number of 0.89, the shock was strongest in this region. This reduction in shock strength is probably due to the isentropic deceleration ahead of the shock associated with induced effect of the fuselage as described in the discussion of the pressure distribution.

There is no perceptible shock on the lower surface at this condition.

Separation.- The pressure recoveries near the trailing edge (fig. 4(g)), the tuft patterns (fig. 7(k)), and the wake measurements (fig. 8(c)) indicate that the separation associated with the onset of the strong shock on the midsemispan region of the upper surface for an angle of attack of 7° at a Mach number of 0.80 is very severe.

These same measurements indicate that the separation on the sections near the tip is negligible, as it is in this region at an angle of attack of 2° at a Mach number of 0.89. As in the case of this lower angle of attack, the elimination of the separation cannot be attributed merely to a reduction of the strength of the shock.

The pressure recoveries, tuft patterns, and wake surveys indicate the presence of considerably less separation at the wing-fuselage juncture than on sections farther outboard. This reduction may be attributed primarily to the same factors that cause a similar reduction at the juncture at an angle of attack of 2° for a Mach number of 0.80. In this case they are also due in part to the fact that the shock in this region is weaker than farther outboard (fig. 8(c)).

Fuselage Pressures

Since the fuselage is cylindrical in the region of the wing-fuselage juncture, it would be expected that the pressure coefficients on the fuselage alone in this region would be relatively small at the various Mach numbers. Therefore, the variations in pressure on the fuselage in this region for the complete configuration as presented in figure 5 indicate the approximate effect of the wing on the fuselage.

For a Mach number of 0.60 and an angle of attack of 2° the induced velocities on the fuselage above and below the wing-fuselage juncture are considerably less than those on the wing at the juncture, as would be expected (fig. 5). The maximum negative pressure coefficient on the upper surface of the fuselage at about the 50-percent-chord station of the juncture is equal to approximately one-half the value at the corresponding station on the wing in this region. The pressure coefficients on the fuselage below the juncture for a Mach number of 0.60 are very nearly equal to zero. The effect of the wing extends at least 25 percent of the juncture chord ahead of the leading edge of the juncture.

When the Mach number is increased from 0.60 to the slightly supercritical value of 0.80 for an angle of attack of 2°, the peak pressure coefficient on the upper surface of the fuselage doubles in magnitude. This increase may be attributed to the rapid expansion of the supersonic field over the upper surface of the wing as indicated by the pressure measured on that surface. Because of this increase, the flow over the upper surface of the fuselage is supersonic for this Mach number.

When the Mach number is increased from 0.80 to 0.89 for an angle of attack of 2°, the peak pressure on the upper surface of the fuselage moves aft and the adverse pressure gradient becomes much more severe. Such changes would be expected in the pressure field above the wing at this Mach number. The highly supersonic Mach number measured ahead of the adverse gradient on the upper surface of the fuselage indicates that the strong shock on the upper surface of the wing should extend around the fuselage at this Mach number. However, the tuft patterns indicate that there is little separation on the fuselage associated with this shock (fig. 7(e)).

The negative pressure coefficients for the lower surface of the fuselage increase markedly when the Mach number is increased to 0.89, as they do on the wing, so that they are slightly supercritical at this Mach number.

CONCLUSIONS

A study of the pressure distributions, wake measurements, and tuft patterns obtained for an unswept, high-aspect-ratio, tapered wing, in conjunction with a fuselage, at high subsonic Mach numbers leads to the following conclusions:

1. When the angle of attack is increased at a Mach number of 0.60, separation occurs initially at the wing-fuselage juncture.

2. Separation associated with the onset of the shock is less severe on the sections of the wing near the tip and wing-fuselage juncture than on the midsemispan sections.

Langley Aeronautical Laboratory
National Advisory Committee for Aeronautics
Langley Air Force Base, Va.

REFERENCES

1. Whitcomb, Richard T.: An Experimental Study at Moderate and High Subsonic Speeds of the Flow over Wings with 30° and 45° of Sweepback in Conjunction with a Fuselage. NACA RM L50K27, 1951

2. Whitcomb, Richard T.: An Experimental Study at Moderate and High Subsonic Speeds of the Flow over Wings with 30° and 45° of Sweepforward in Conjunction with a Fuselage. NACA RM L50K28, 1951

3. Whitcomb, Richard T.: Investigation of the Characteristics of a High-Aspect-Ratio Wing in the Langley 8-Foot High-Speed Tunnel. NACA RM L6H28a, 1946.

4. Whitcomb, Richard T.: A Compilation of the Pressures Measured on a Wing and Aileron with Various Amounts of Sweep in the Langley 8-Foot High-Speed Tunnel. NACA RM L8A30a, 1948.

5. Baals, Donald D., and Mourhess, Mary J.: Numerical Evaluation of the Wake-Survey Equations for Subsonic Flow Including the Effect of Energy Addition. NACA ARR L5H27, 1945.

6. Hess, Robert V., and Gardner, Clifford S.: Study by the Prandtl-Glauert Method of Compressibility Effects and Critical Mach Number for Ellipsoids of Various Aspect Ratios and Thickness Ratios. NACA TN 1792, 1949.

7. Stack, John, and Lindsey, W. F.: Characteristics of Low-Aspect-Ratio Wings at Supercritical Mach Numbers. NACA Rep. 922, 1949.

8. Whitcomb, Richard T.: An Investigation of the Effects of Sweep on the Characteristics of a High-Aspect-Ratio Wing in the Langley 8-Foot High-Speed Tunnel. NACA RM L6J01a, 1947.

9. Ackeret, J., Feldmann, F., and Rott, N.: Investigations of Compression Shocks and Boundary Layers in Gases Moving at High Speed. NACA TM 1113, 1947.

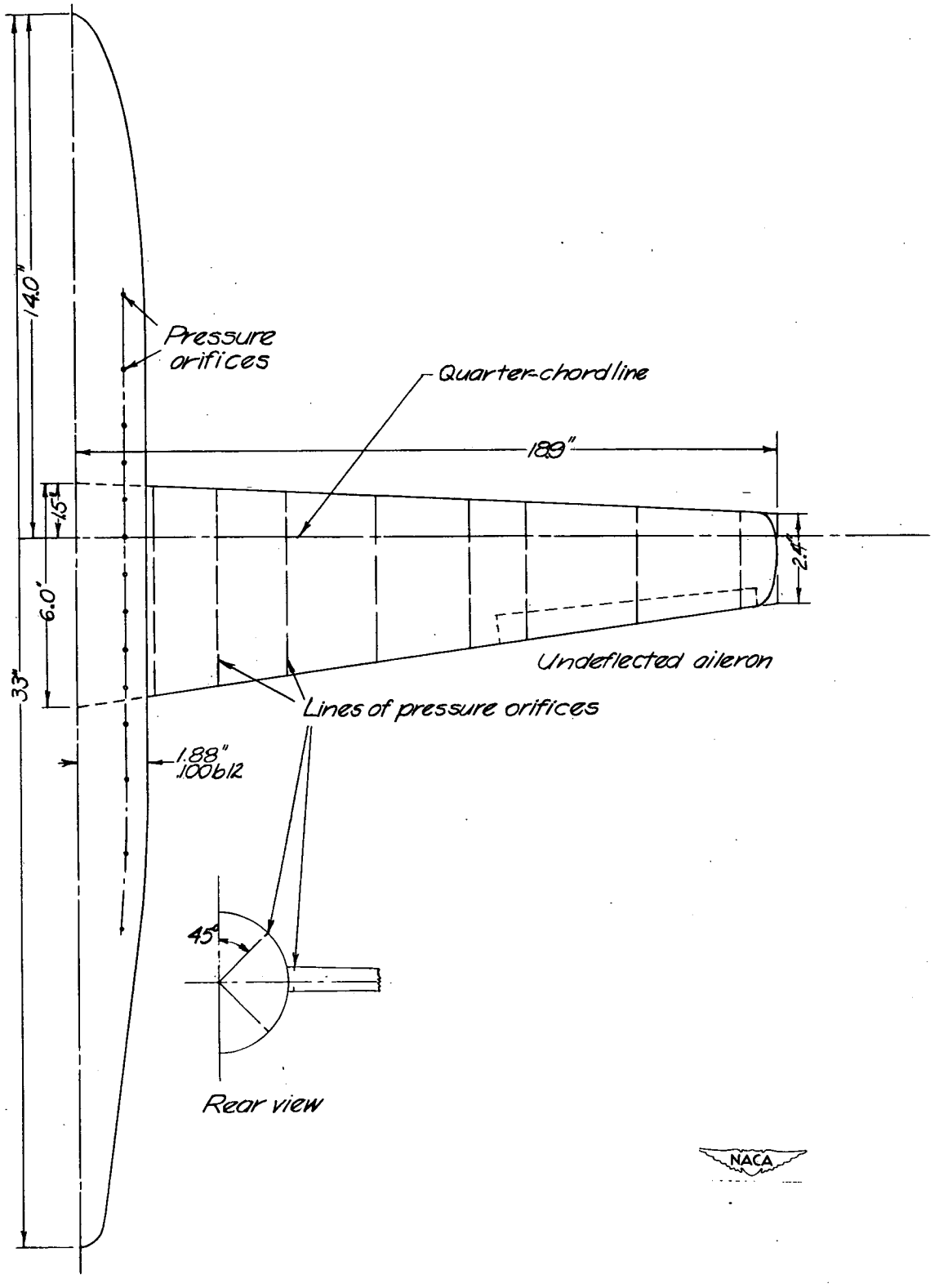

Figure 1.- Configuration.

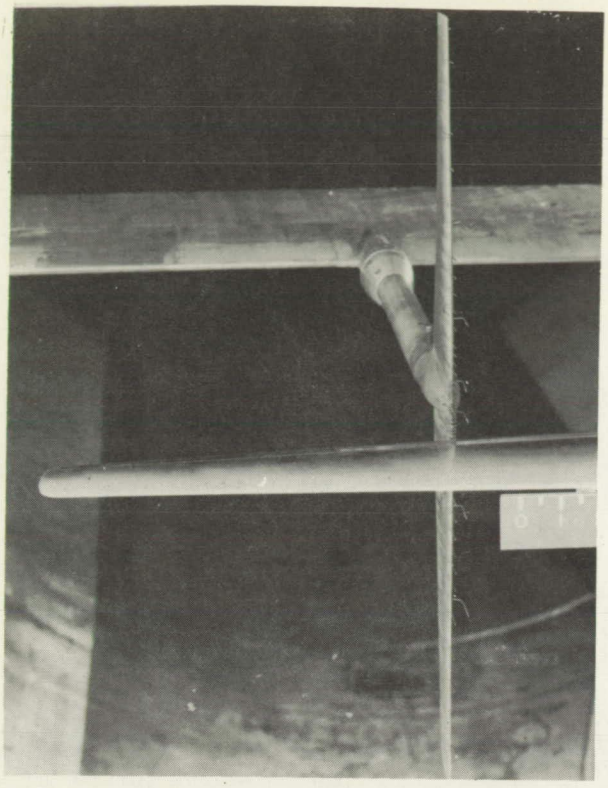

Figure 2.- Wake-survey rake.

L-43593

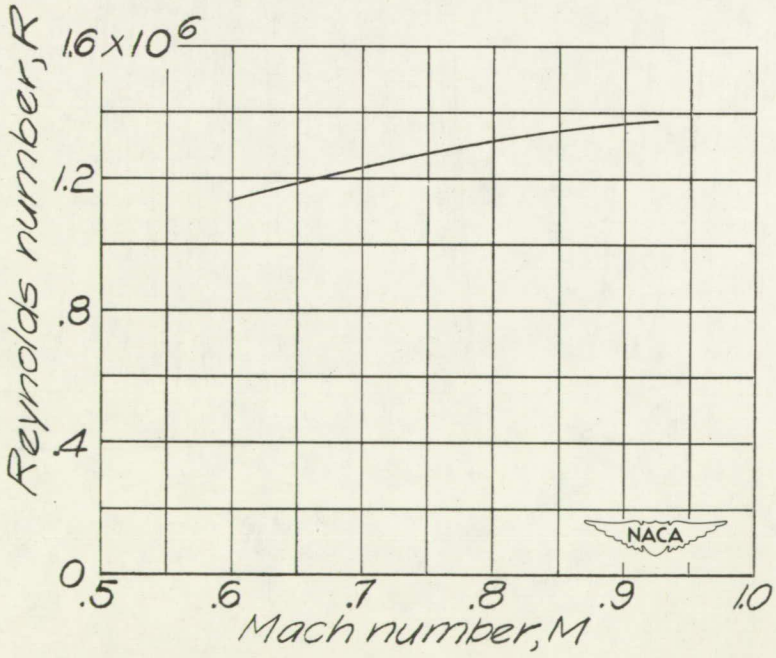

Figure 3.- Variation of Reynolds number with Mach number.

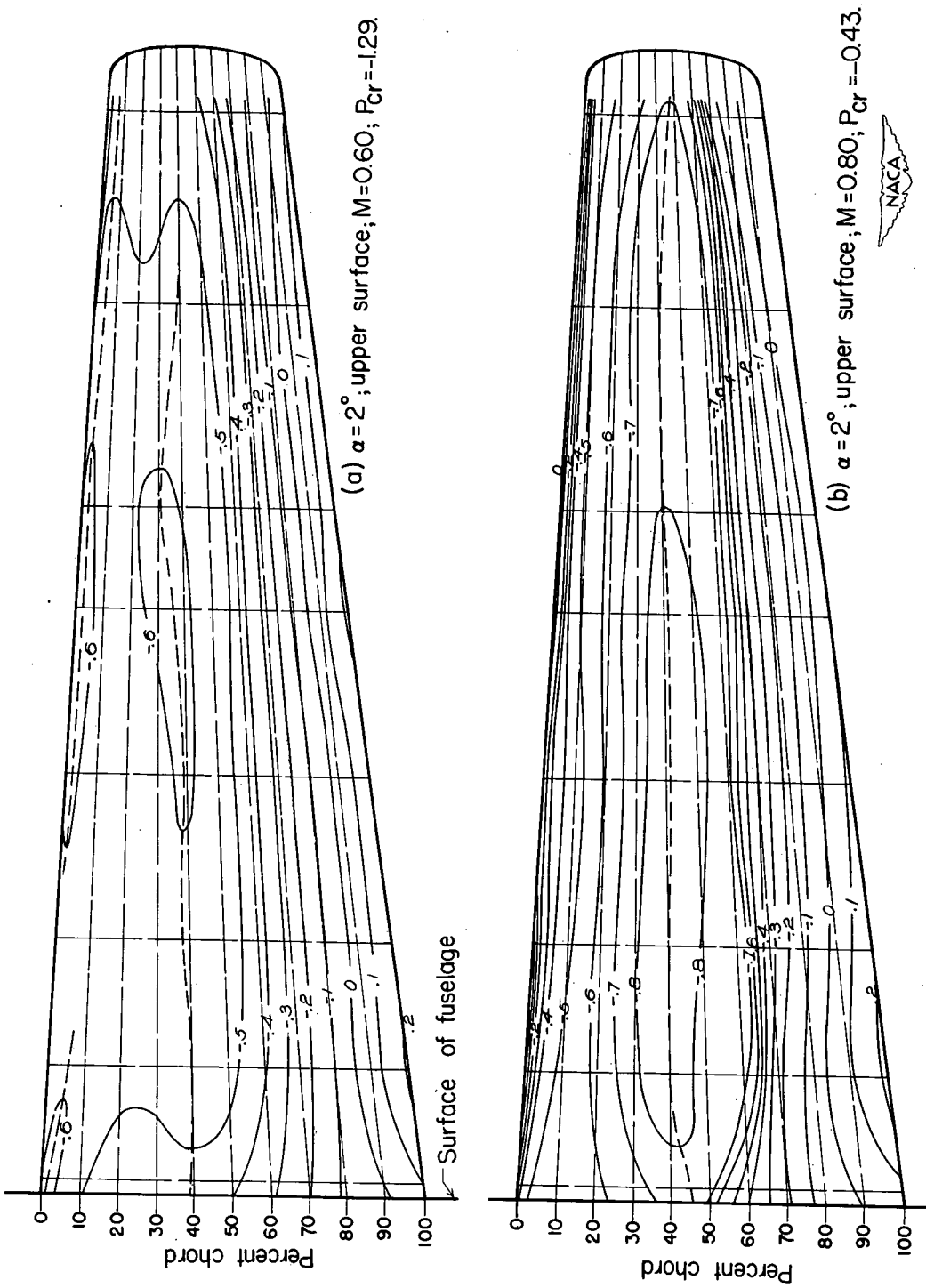

Figure 4.- Equal-pressure-coefficient contours.

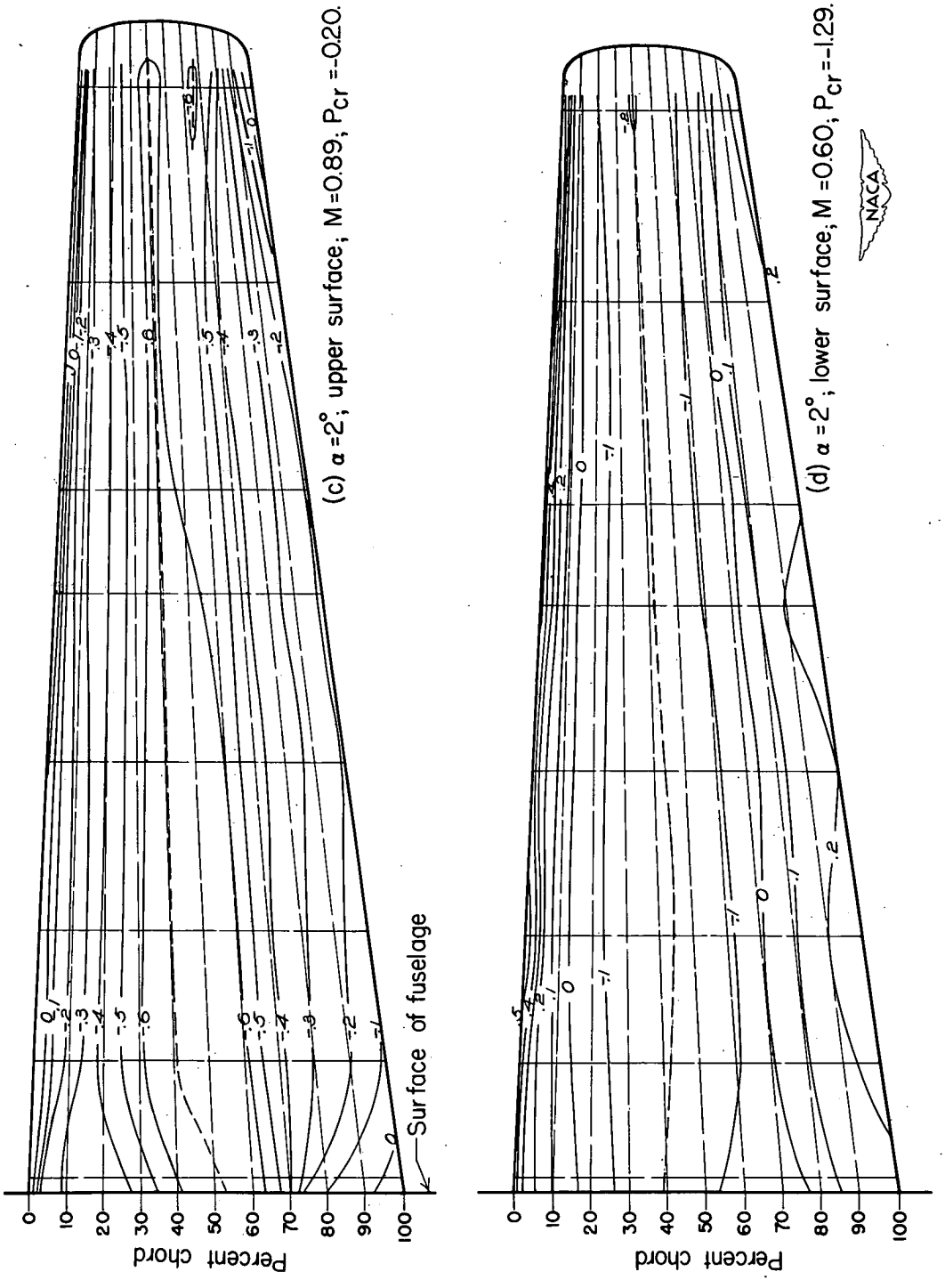

Figure 4.- Continued.

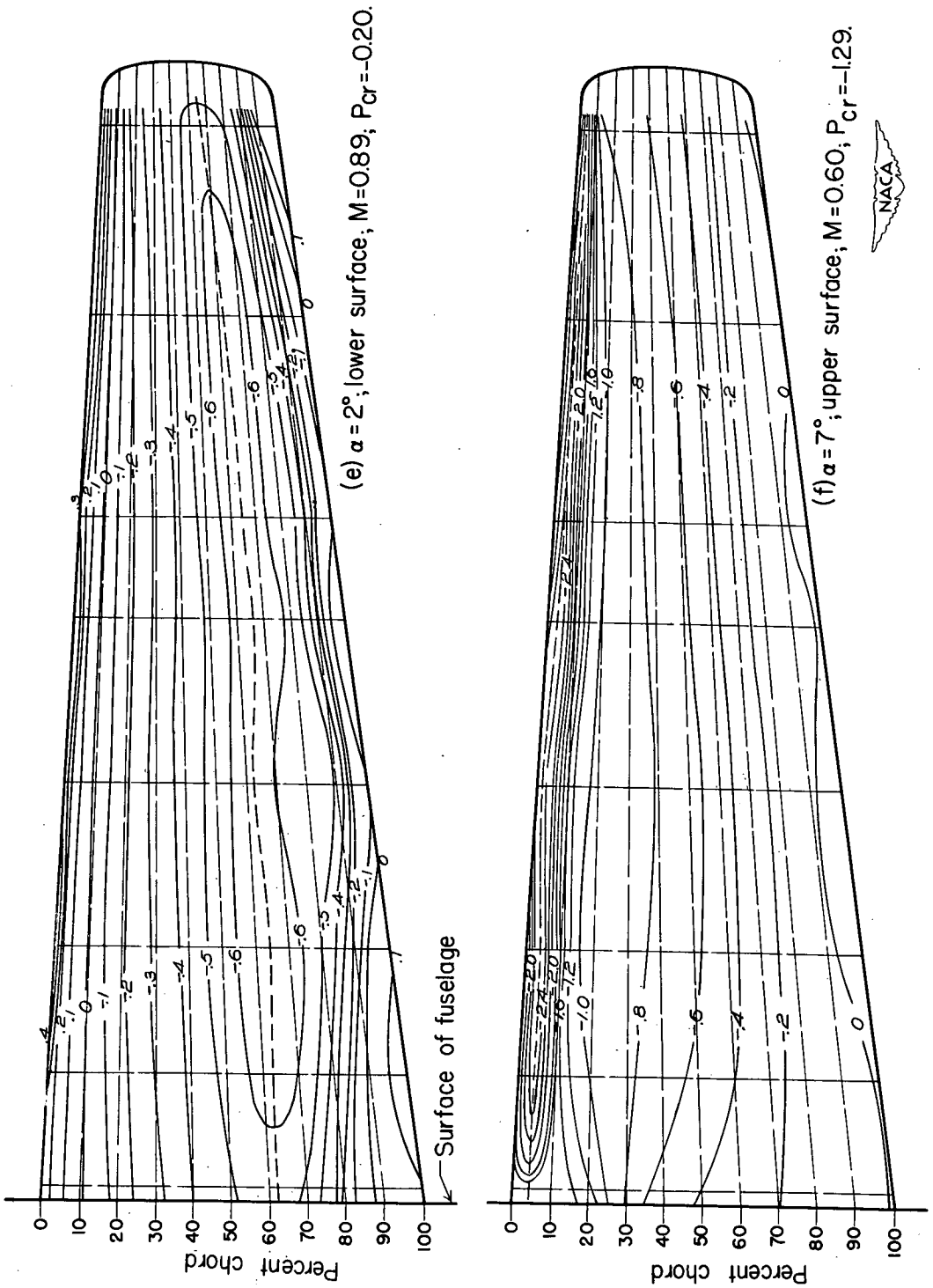

Figure 4.- Continued.

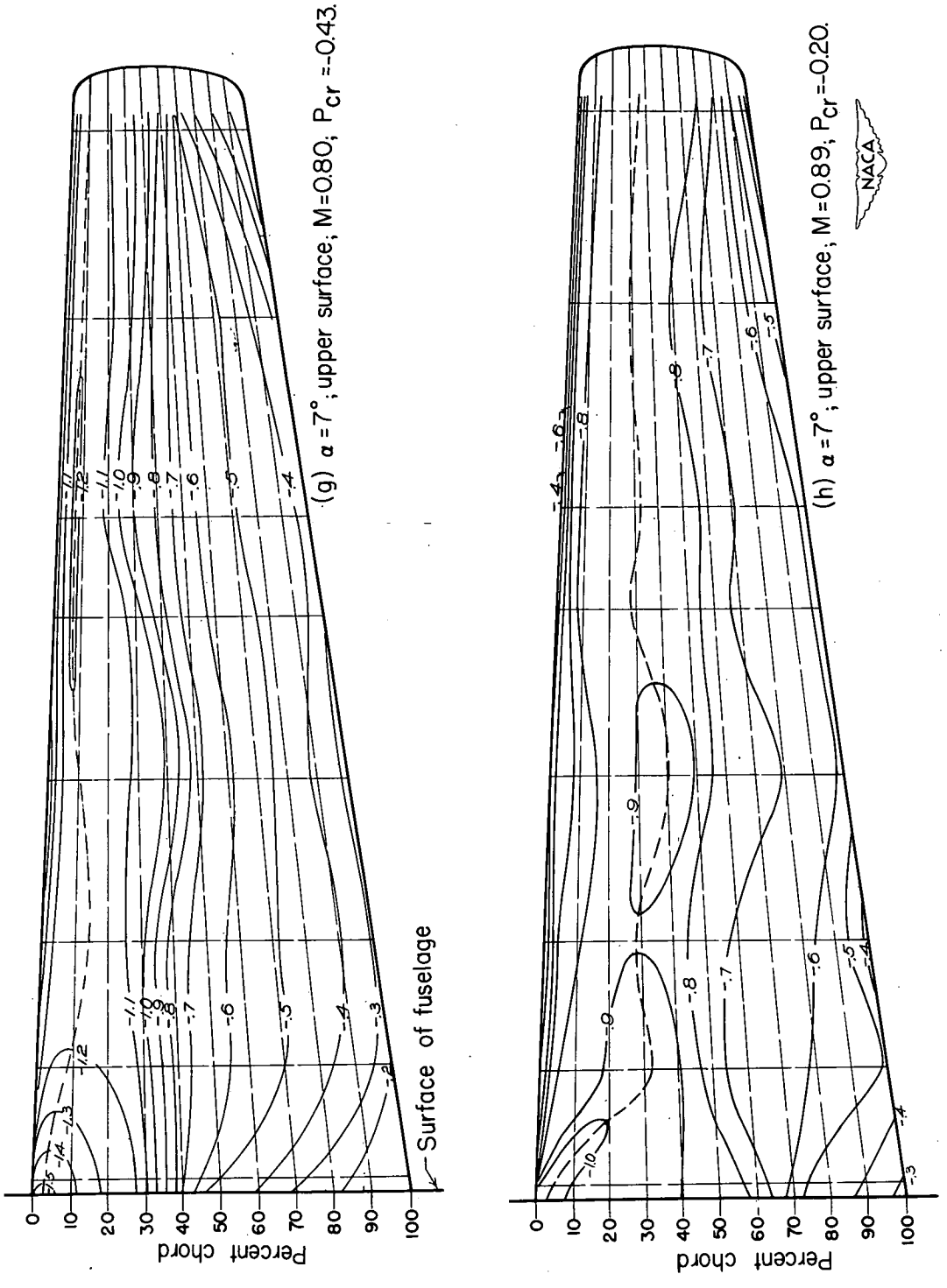

Figure 4.- Continued.

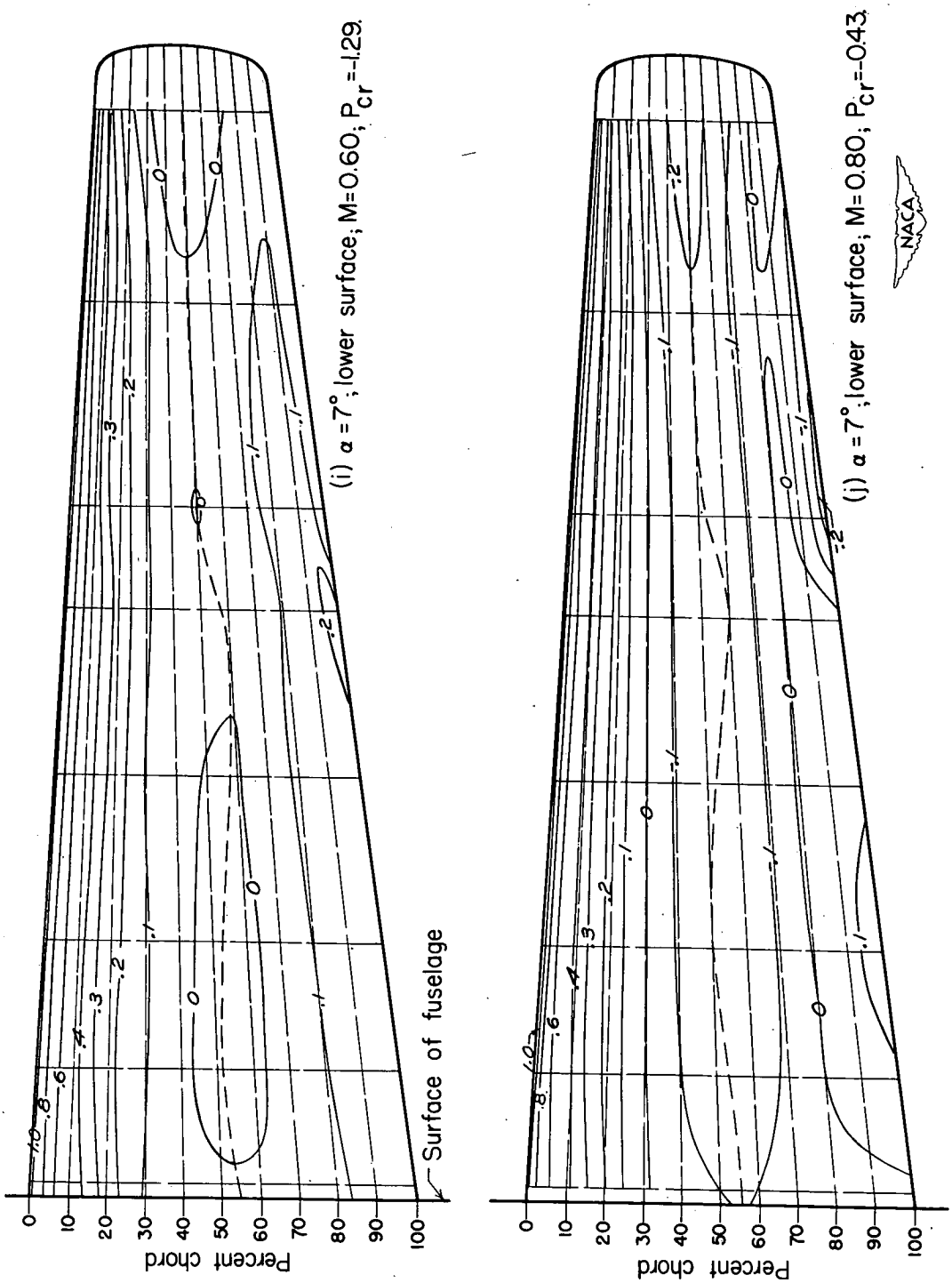

Figure 4.- Concluded.

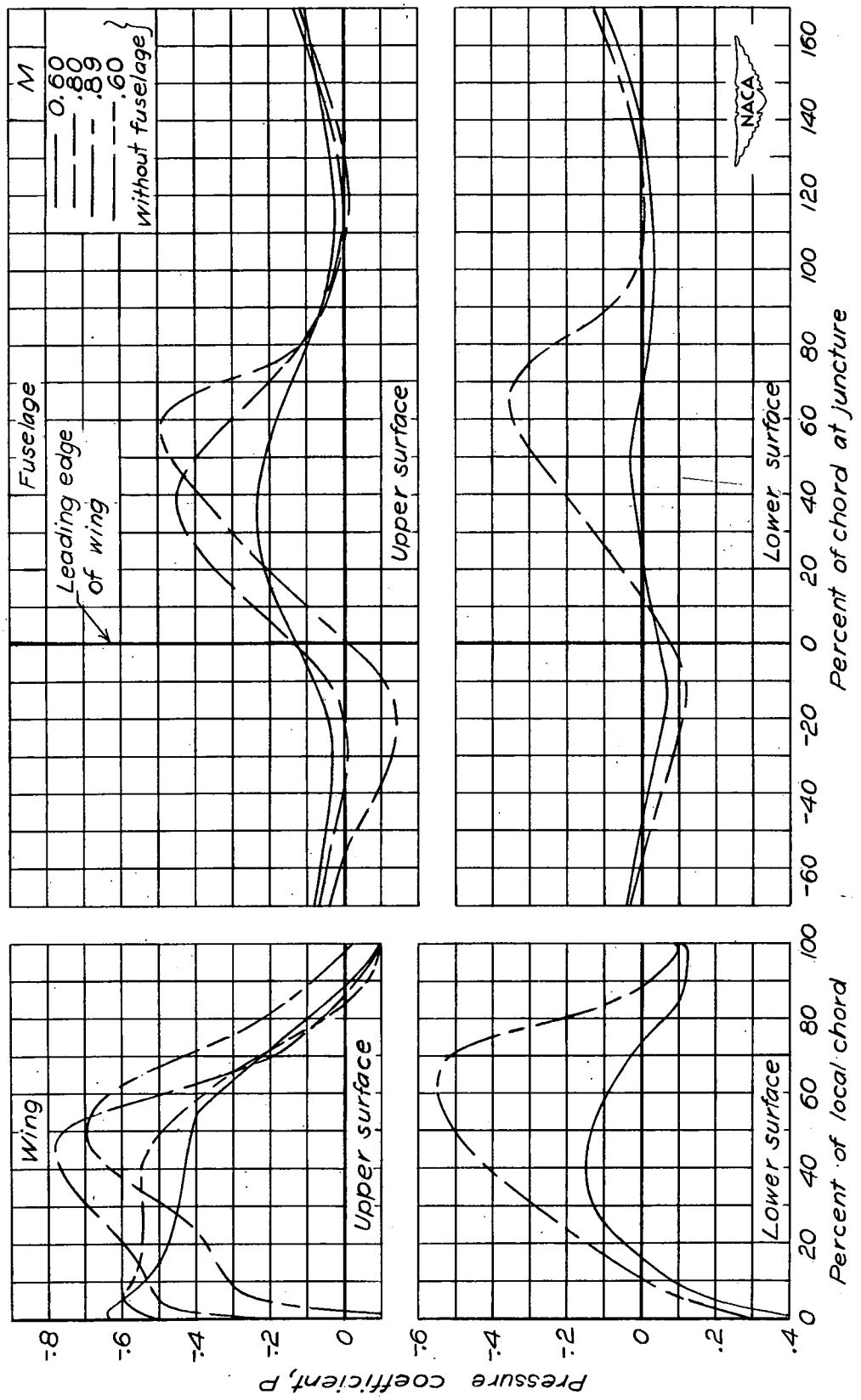

(a) $\alpha = 2^{\circ}$.

Figure 5.- Chordwise pressure distributions near wing-fuselage juncture.

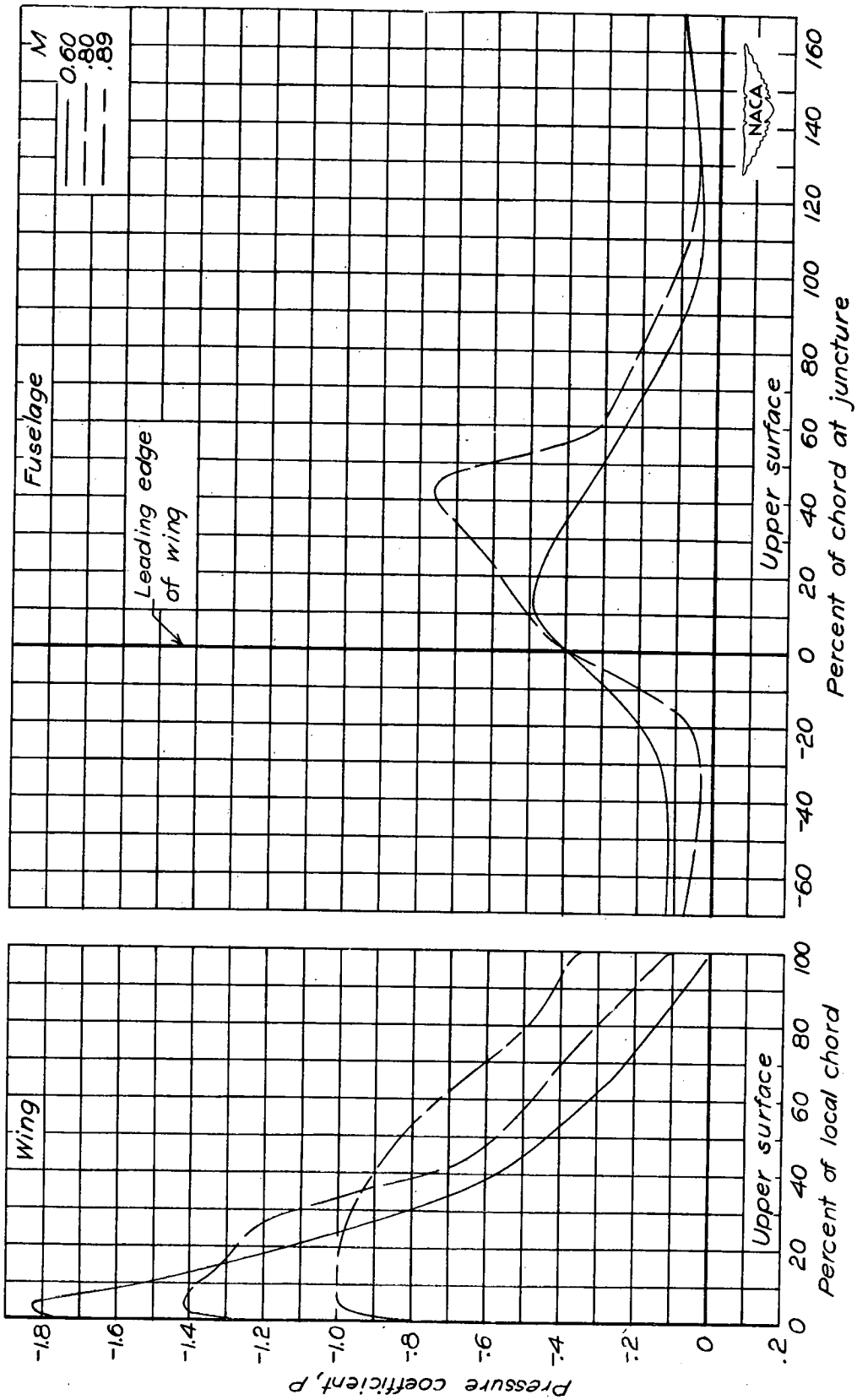

(b) $\alpha = 7^{\circ}$.

Figure 5.- Concluded.

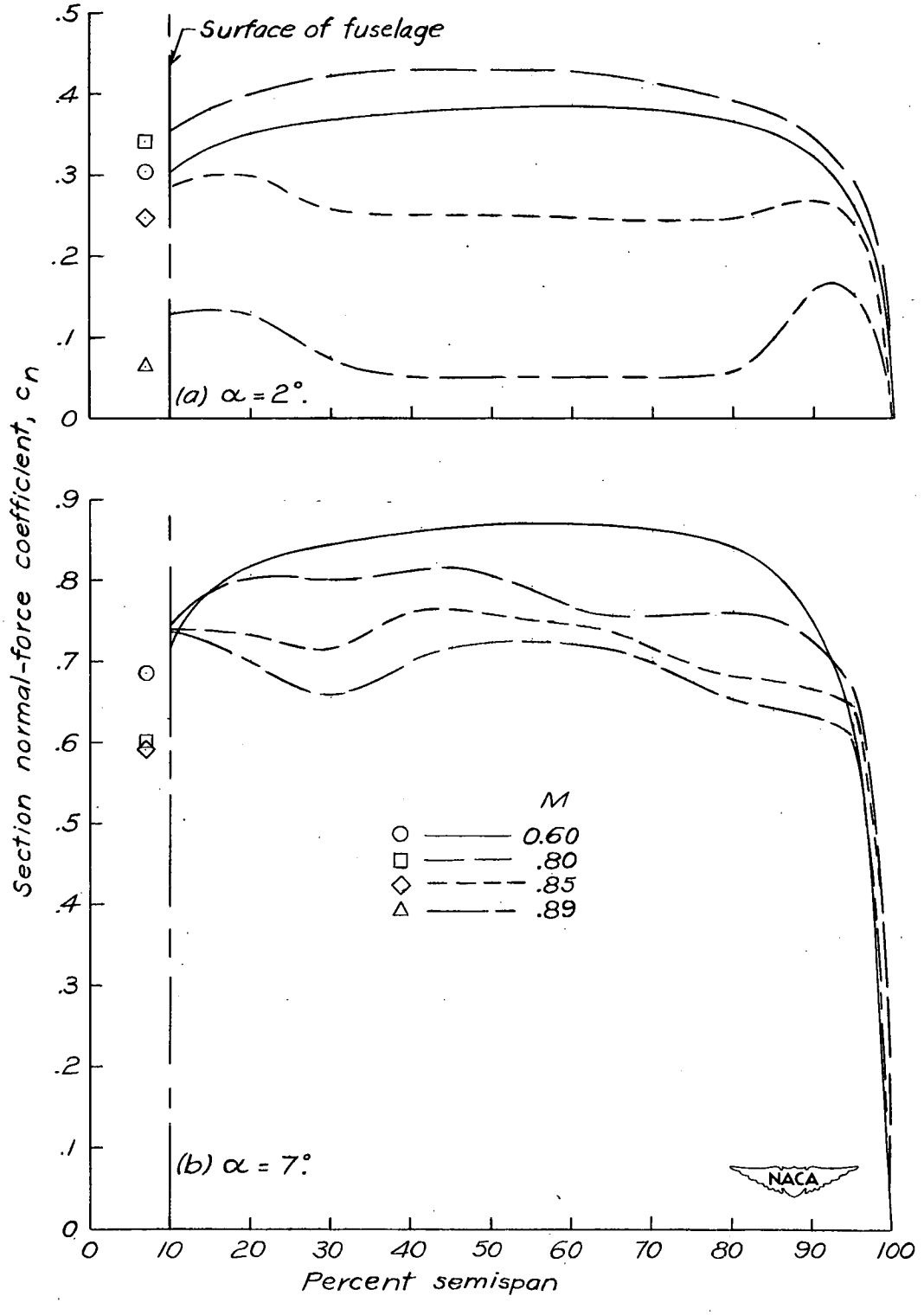

Figure 6.- Spanwise variations of section normal-force coefficient on wing-fuselage combination for various Mach numbers. (Symbols refer to data obtained at station on fuselage.)

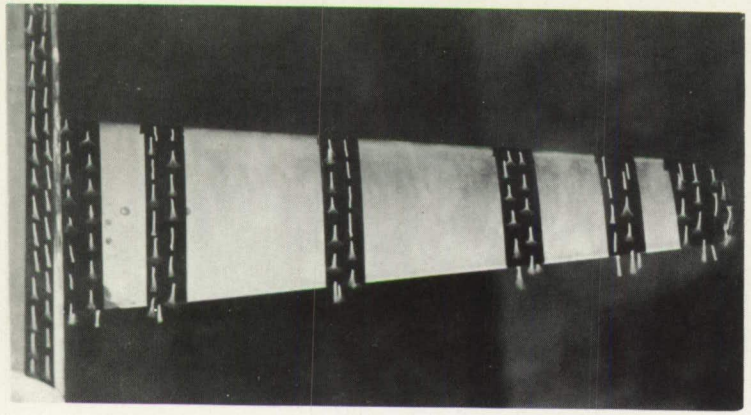

(a) $\alpha = 2^{\circ}$; upper surface; M = 0.60.

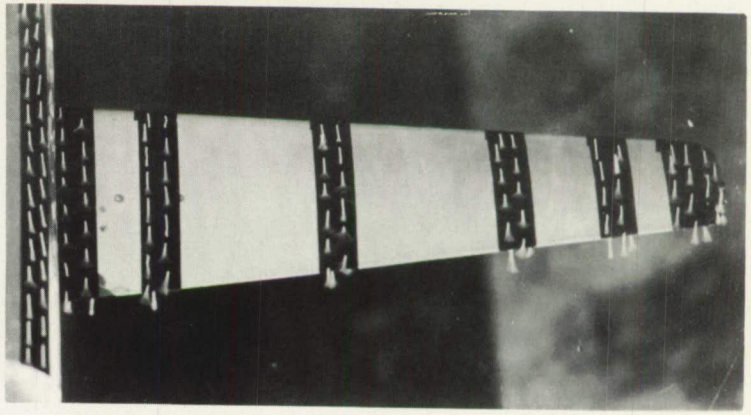

(b) $\alpha = 2^{\circ}$; upper surface; M = 0.75.

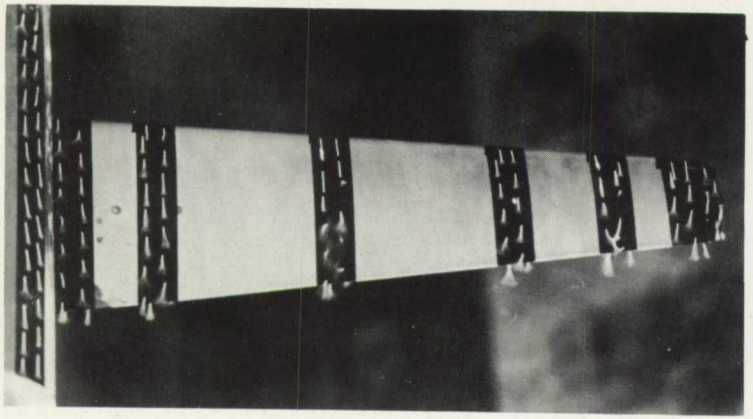

(c) $\alpha = 2^{\circ}$; upper surface; M = 0.80.

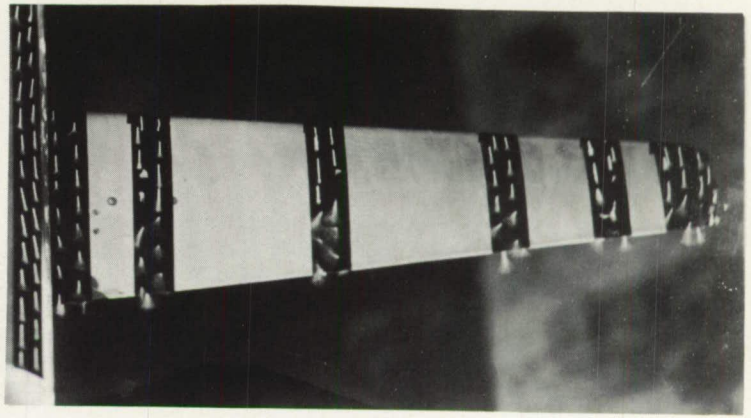

(d) $\alpha = 2^{\circ}$; upper surface; M = 0.85.

Figure 7.- Tuft patterns on unswept wing.

NACA
L-67976

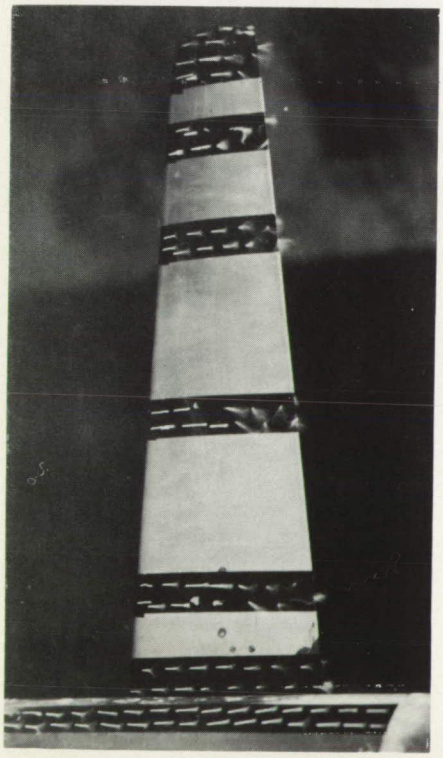

(e) $\alpha = 2^{\circ}$; upper surface; M = 0.89.

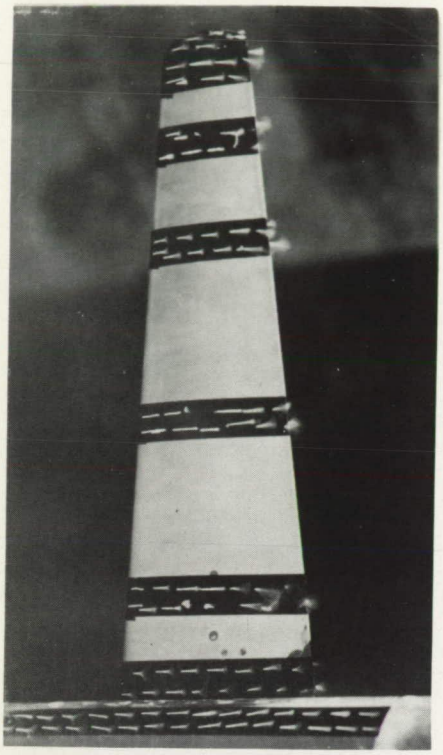

(f) $\alpha = 2^{\circ}$; upper surface; M = 0.925.

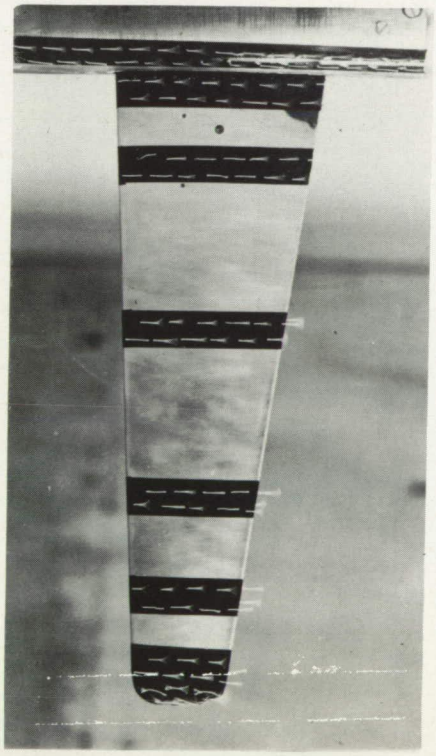

(g) $\alpha = 2^{\circ}$; lower surface; M = 0.60.

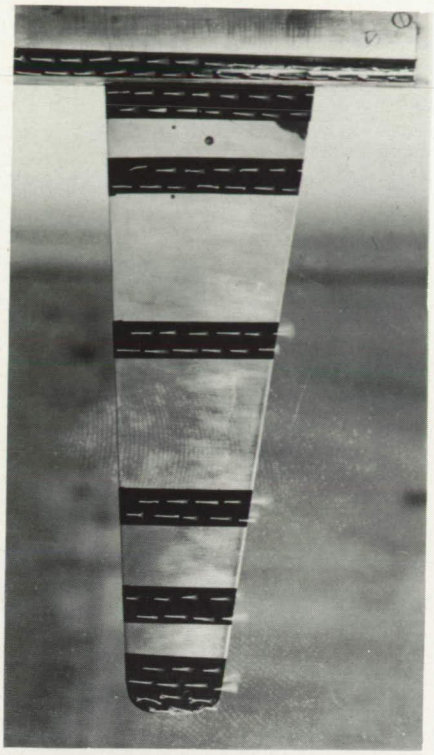

(h) $\alpha = 2^{\circ}$; lower surface; M = 0.925.

Figure 7.- Continued.

L-67977

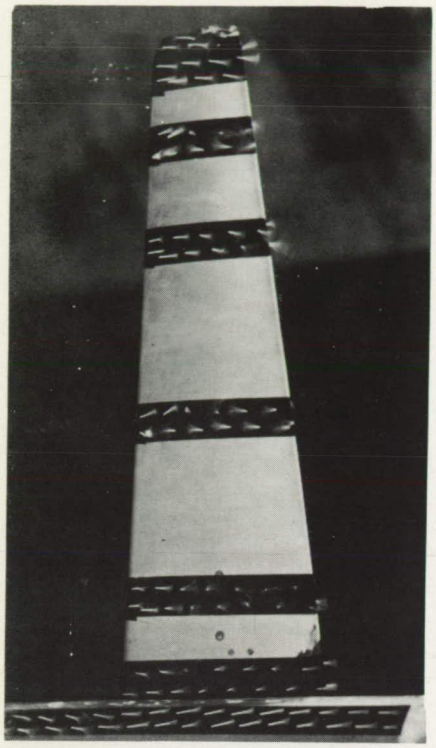

(j) $\alpha = 7^{\circ}$; upper surface; M = 0.75.

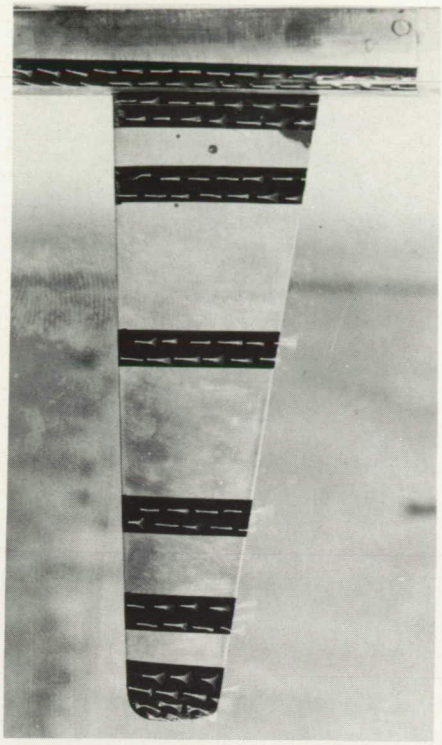

(l) $\alpha = 7^{\circ}$; lower surface; M = 0.60.

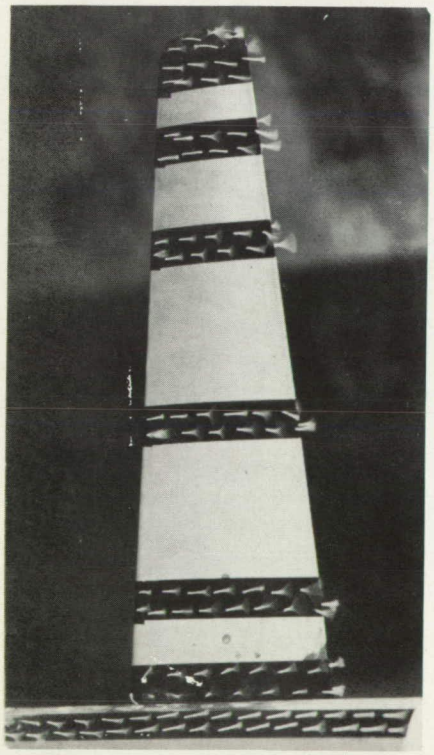

(i) $\alpha = 7^{\circ}$; upper surface; M = 0.60.

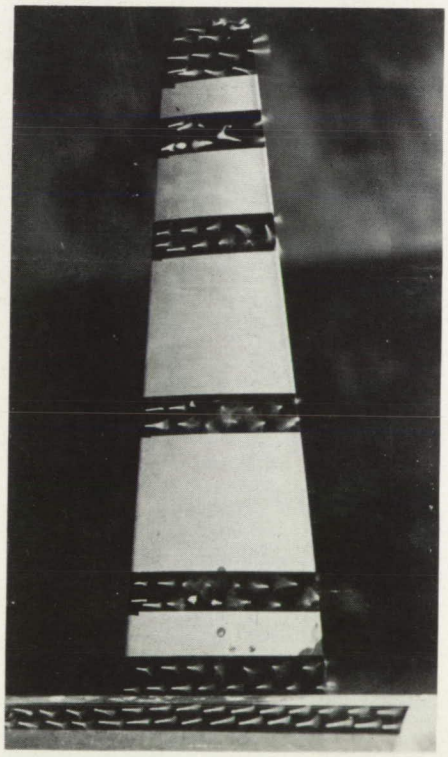

(k) $\alpha = 7^{\circ}$; upper surface; M = 0.80.

Figure 7.- Concluded.

L-67978

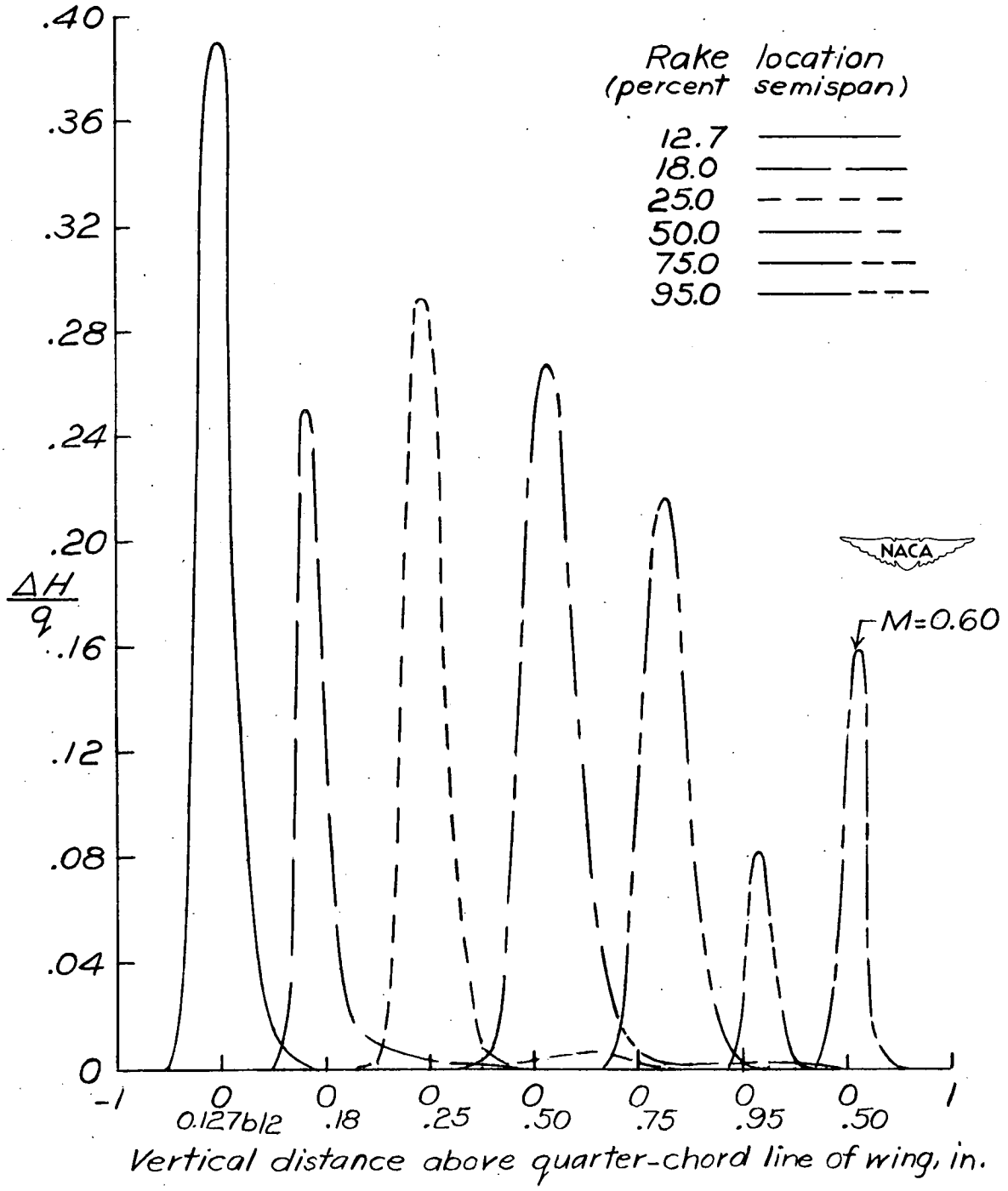

(a) $\alpha = 2^{\circ}$; $M = 0.80$.

Figure 8.- Wake profiles at various spanwise vertical survey positions.

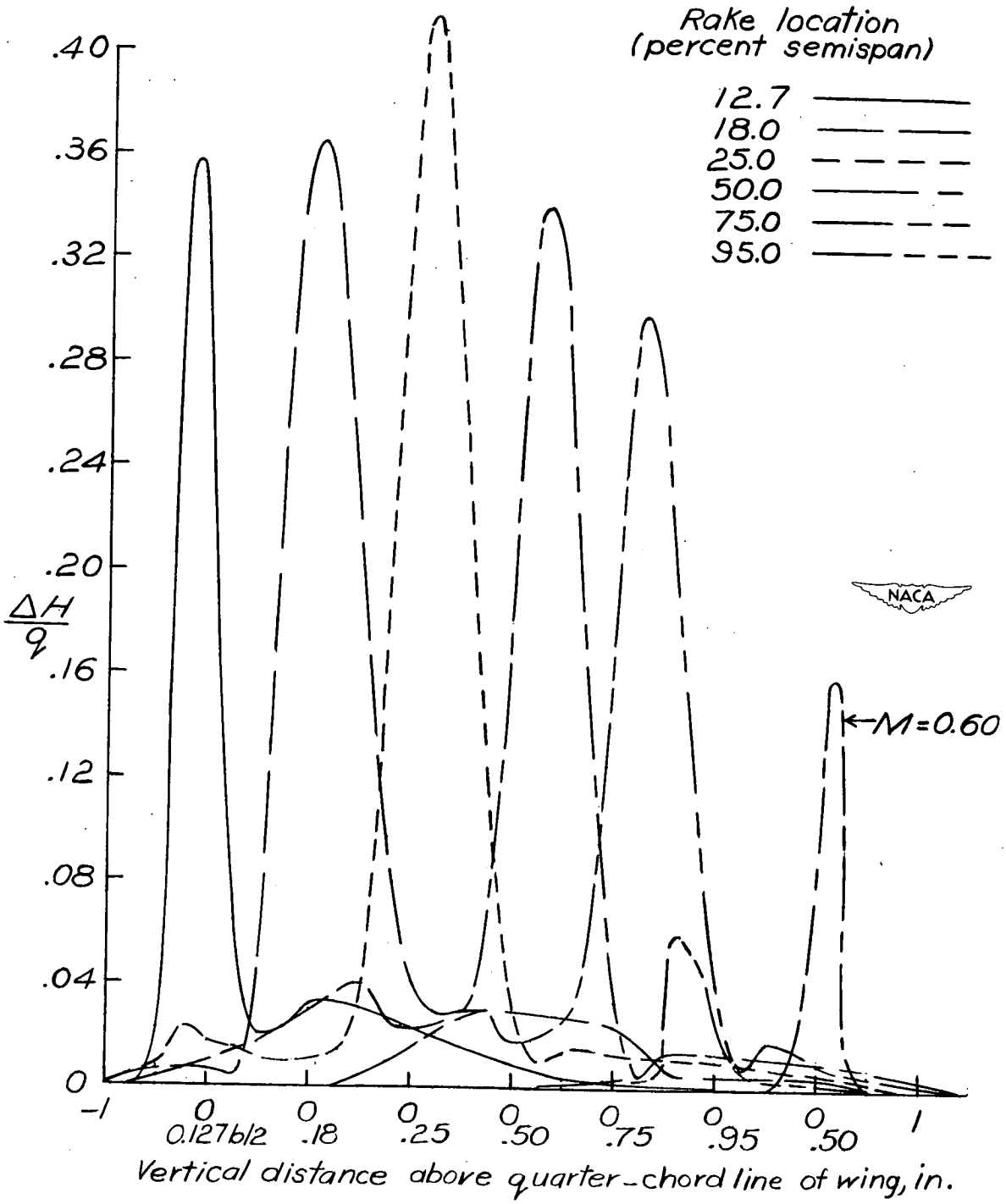

(b) $\alpha = 2^{\circ}$; $M = 0.89$.

Figure 8.- Continued.

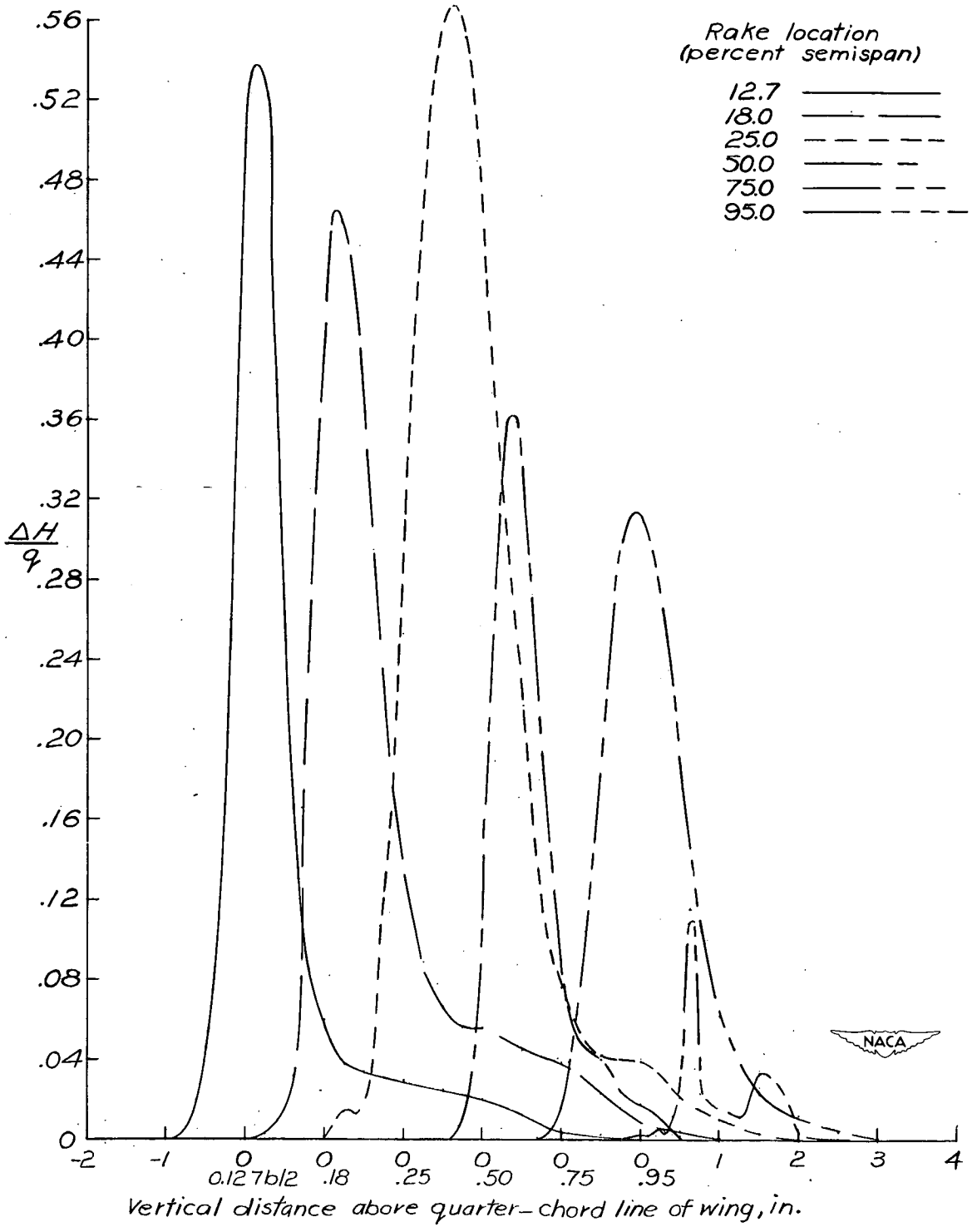

(c) $\alpha = 7^{\circ}$; M = 0.80.

Figure 8.- Concluded.

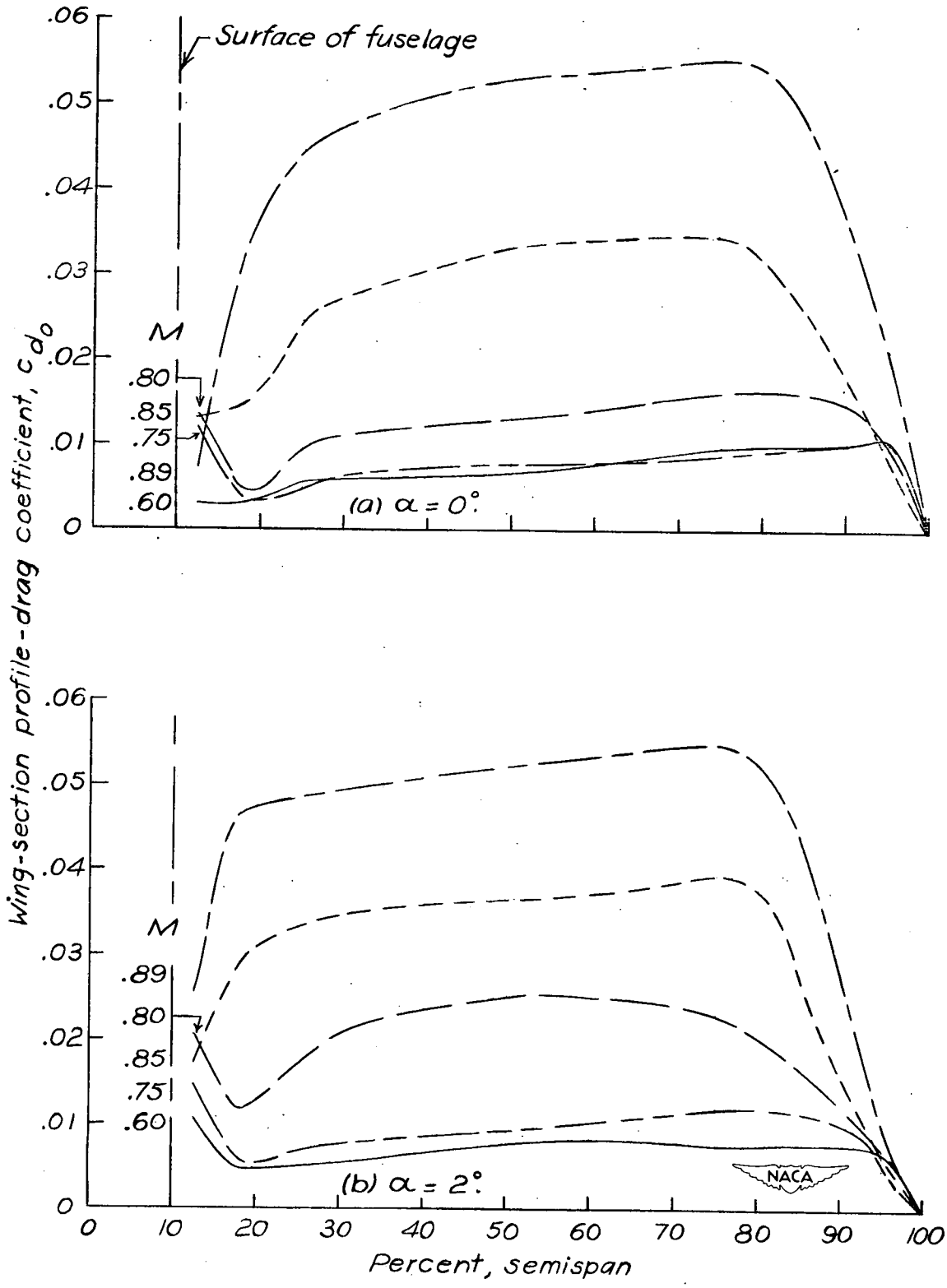

Figure 9.- Spanwise variations of wing-section profile-drag coefficient for various Mach numbers.

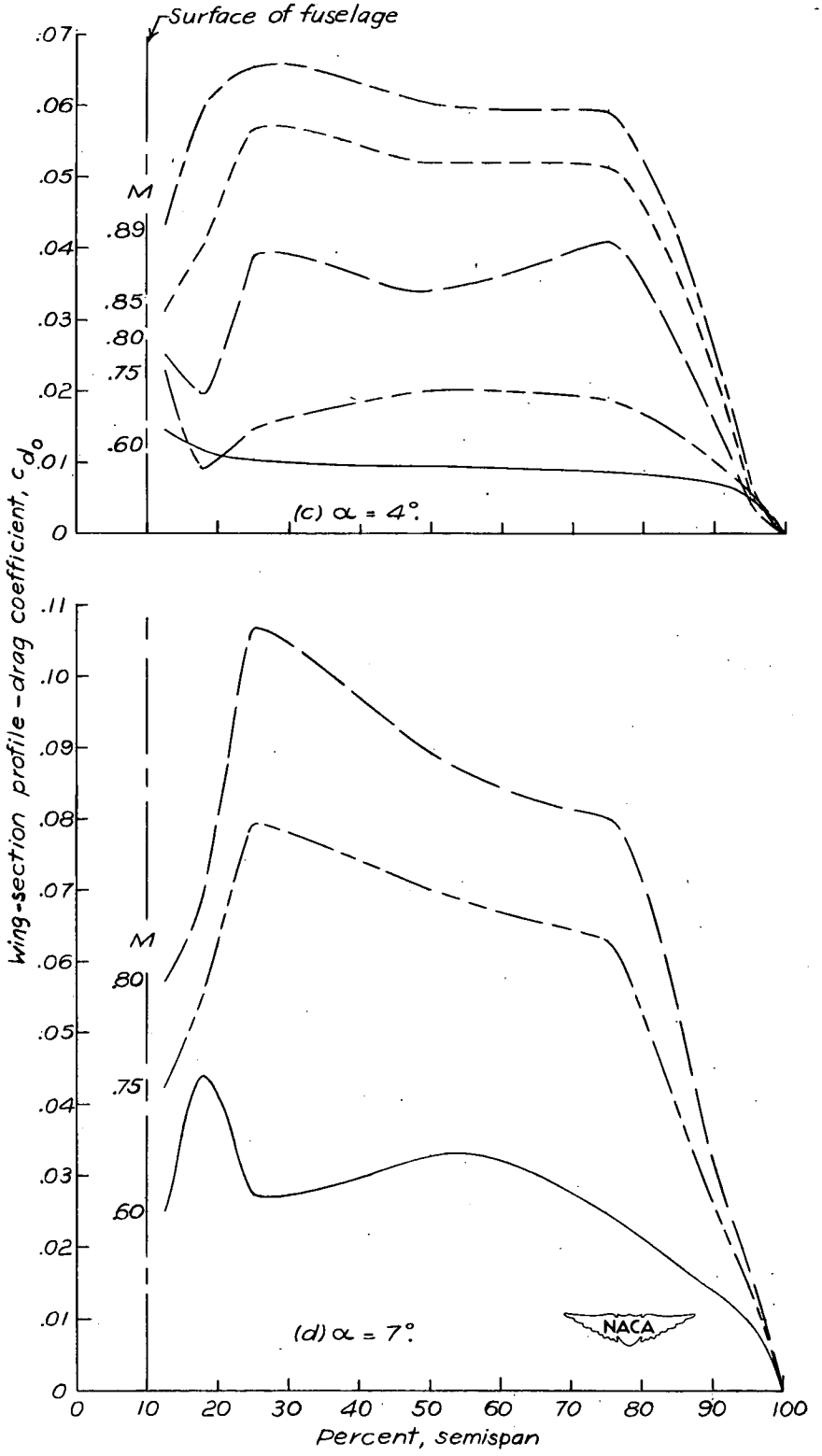

Figure 9.- Concluded.